JOURNAL OF CHEMICAL INFORMATION AND MODELING

Article

pubs.acs.org/jcim

New Insights on the Reaction Pathway Leading to Lactyl-ThDP: A Theoretical Approach

Ignacio Lizana,[†] Gonzalo A. Jaña,[‡] and Eduardo J. Delgado*[,†]

[†]Computational Chemistry Group, Faculty of Chemical Sciences, Universidad de Concepción, Concepción, Chile

[‡]Departamento de Ciencias Químicas, Facultad de Ciencias Exactas, Sede Concepción, Universidad Andrés Bello, Concepción, Chile

ABSTRACT: In all ThDP-dependent enzymes, the catalytic cycle is initiated with the attack of the C_2 atom of the ylide intermediate on the C_α atom of a pyruvate molecule to form the lactyl-ThDP (L-ThDP) intermediate. In this study, the reaction between the ylide intermediate and pyruvate leading to the formation of L-ThDP is addressed from a theoretical point of view. The study includes molecular dynamics, exploration of the potential energy surface by means of QM/MM calculations, and reactivity analysis on key centers. The results show that the reaction occurs via a concerted mechanism in which the carboligation and the proton transfers occur synchronically. It is also observed that during the reaction the protonation state of the N1′ atom changes: the reaction starts with the ylide having the N1′ atom deprotonated and reaches a transition state showing the N1′ atom protonated. This conversion leads to the reaction path of minimum energy, with an activation energy of about 20 kcal mol^{-1}. On the other hand, it is also observed that the approaching distance between the pyruvate and the ylide, i.e., the C_α−C_2 distance, plays a fundamental role in the reaction mechanism since it determines the nucleophilic character of key atoms of the ylide, which in turn trigger the elemental reactions of the mechanism.

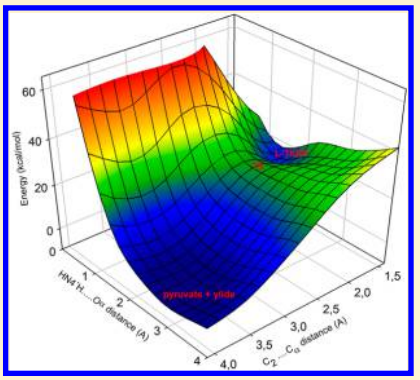

INTRODUCTION

Acetohydroxy acid synthase (AHAS) is a thiamin diphosphate (ThDP)-dependent enzyme involved in the biosynthesis of branched-chain amino acids (valine, leucine, and isoleucine) in plants, bacteria, and fungi. The ThDP cofactor is composed of two aromatic rings, a 4-aminopyrimidine ring and a thiazolium ring, bridged by a methylene group. According to the literature, during catalysis by ThDP-dependent enzymes the 4-amino-pyrimidine moiety can interconvert among four ionization/tautomeric states: the 4′-aminopyrimidine (AP), the N1′-protonated 4′-aminopyrimidium ion (APH$^+$), the 1′,4′-iminopyrimidine (IP), and the C_2-ionized ylide (Y).[1−3]

The catalytic cycle of AHAS is initiated with the attack of the C_2 atom of the ylide intermediate on the C_α atom of a pyruvate molecule to form the lactyl-ThDP (L-ThDP) intermediate, which then undergoes decarboxylation to form the hydroxyethyl thiamin diphosphate (HEThDP) enamine/carbanion. Afterward, HEThDP reacts with a second molecule of an α-keto acid (pyruvate or 2-ketobutyrate) to form the intermediate AHA-ThDP, which finally leads to release of the product and the recovery of the ylide.[4−7]

Because of its ability to form asymmetric carbon−carbon bonds, AHAS is a versatile catalyst for the stereoselective synthesis of nonphysiological products of interest in the pharmaceutical industry.[8−10] Thus, AHAS has been described as an efficient catalyst for the synthesis of (*R*)-phenylacetylcarbinol (R-PAC), an important pharmaceutical precursor for the synthesis of a variety of drugs with β-adrenergic agonist/antagonist properties. Therefore, detailed mechanistic and structural insights are required in order to tailor the enzyme for the chiral synthesis of the nonphysiological product R-PAC. On the other hand, a detailed knowledge of the mechanism is also essential for the development of novel inhibitors of the enzyme, used as herbicides and bactericides, which act by interrupting the catalytic cycle and preventing the synthesis of acetolactate and 2-keto-2-hydroxybutyrate, intermediates in the biosynthetic pathway toward the synthesis of branched amino acids, in this way causing the death of the organism (plant or microorganism) by the lack of these amino acids.

Despite the number of articles published on the catalytic cycle of AHAS, there are still some aspects that remain unknown or controversial.[11,12] Specifically in regard to the formation of the L-ThDP intermediate, there are some issues that remain unclear, namely, the manner in which the reaction occurs (i.e., via a stepwise or concerted mechanism) and the protonation states of the N1′ atom and the N atom of the C4′ amino group (from now on called the N4′ atom) during the attack of the C_2 atom on the pyruvate C_α atom.

In previous articles[13,14] we studied the formation of L-ThDP considering a simplified model including only the pyruvate molecule and the conserved side chain of glutamic acid interacting with the N1′ atom of ThDP. In addition, in order to simplify the calculations, the diphosphate group of ThDP was replaced with a hydroxyl group and the side chains were ignored except for the mentioned glutamic acid, which was replaced by acetic acid. The results allowed us to conclude that the reaction leading to the formation of L-ThDP occurs via a

Received: April 10, 2015
Published: July 29, 2015

DOI: 10.1021/acs.jcim.5b00197
J. Chem. Inf. Model. 2015, 55, 1640−1644

concerted mechanism and that during the nucleophilic attack on the pyruvate molecule the N1′ atom of the ylide remains deprotonated.

In the current study, we investigate the formation of the L-ThDP intermediate from a theoretical point of view, considering the total proteic ambient. The study includes molecular dynamics simulations, exploration of the potential energy surface (PES) by means of QM/MM calculations, and reactivity analysis on key centers of the reacting species. We postulate that the ylide intermediate itself can act as the proton donor (Figure 1), in line with our previous articles, in this way

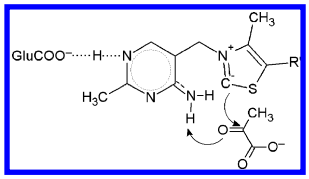

Figure 1. Proposed mechanism for the formation of L-ThDP.

avoiding the involvement of any additional acid−base ionizable group. The PESs are explored for both forms of the ylide, namely, that having the N1′ atom deprotonated and that having the N1′ atom protonated (from now on called the Y_1 and Y_2 forms, respectively). The exploration of the PES is carried out in terms of two reaction coordinates accounting for the carboligation and proton transfer.

METHODOLOGY

The crystal structure of AHAS from *Saccharomyces cerevisiae* yeast in complex with the chlorimuron ethyl herbicide determined at 2.8 Å (PDB code 1N0H) was used as the starting structure. The herbicide was replaced by pyruvate, superimposing the carbonyl carbon of pyruvate on the carboxylic carbon of the herbicide, which in turn was deleted.

The initial AHAS−ylide−pyruvate structure for the exploration of the PES was obtained from the solvated and equilibrated structure of the complex after a 20 ns molecular dynamics (MD) simulation performed according to methodology described earlier.[15,16] The obtained plot of root-mean-square deviation (RMSD) versus simulation time (Figure 2) assured the stability of the complete system at the above considered simulation time.

During the simulation, no significant displacement of the amino acids located in the active site was observed. Thus, the final MD structure was taken as a single representative configuration to model the reaction pathway. This starting configuration was trimmed to a sphere of 33 Å centered on C_2 of the ylide. The system was partitioned into a QM region consisting of the ylide intermediate, pyruvate, and the residues Arg380 and Glu139, whereas the MM region contained the rest of the system. The inclusion of the above residues in the QM subsystem was supported by our previous results and experimental evidence.

The proposed mechanism was described on the PES in terms of the two reaction coordinates R_1 and R_2, where R_1 is defined as the C_2-C_α distance, to account for the carboligation between the C_2 atom of the ylide and the C_α atom of pyruvate, whereas R_2 is defined as the $H-O_\alpha$ distance, to account for the proton transfer from the N4′ atom to the carbonyl oxygen of pyruvate (Figure 3).

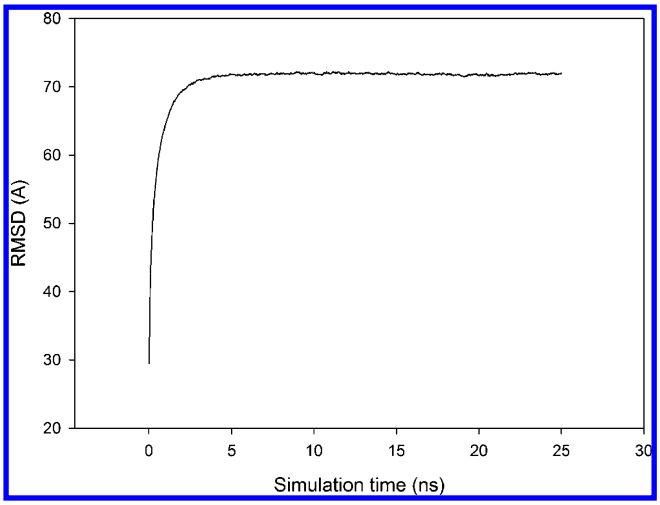

Figure 2. Plot of distance root-mean-square deviation (RMSD) vs simulation time.

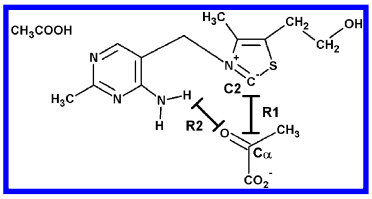

Figure 3. Reaction coordinates considered for the exploration of the PES.

The CHARMM program was employed to carry out the PES exploration by means of a series of geometry optimizations of the mobile part of the system in the presence of harmonic restraints (RESD module) applied on the two reaction coordinates previously defined. The QM subsystem was described with the AM1 Hamiltonian, and the link-atom approach was applied to the boundary atoms. The CHARMM27 all-atoms force field was used to describe the rest of the atoms in the 33 Å sphere. The use of the AM1 Hamiltonian in QM/MM studies has been reported to provide optimized geometries comparable to those obtained using higher levels of theory.[17] Along the optimizations, those atoms located 25 Å away from the C_2 atom of the ylide were kept frozen. Each energy minimization was carried out with a gradient tolerance of 0.001 kcal mol^{-1} using the ABNR algorithm.

Afterward, the AM1/MM potential energy surface was corrected with high-level single-point energy calculations (B3LYP-D3/6-31+G(d,p)) for each optimized structure obtained from the AM1/MM calculations. Grimme corrections were incorporated in order to include the effect of dispersive (van der Waals) forces in the study. All of these calculations were carried out using CHARMM[18] and Q-CHEM[19] software. The reactivity analysis was performed by calculating Fukui reactivity indices on key atoms using the methodology implemented in Jaguar.[20]

RESULTS AND DISCUSSION

Potential Energy Surfaces. The PESs for the two forms of the ylide, Y_1 and Y_2, were explored by variation of the two reaction coordinates between about 1.0 and 4.0 Å (Figures 4 and 5). The PESs so obtained show very similar topologies, having three critical points that are associated with reactants

DOI: 10.1021/acs.jcim.5b00197
J. Chem. Inf. Model. 2015, 55, 1640−1644

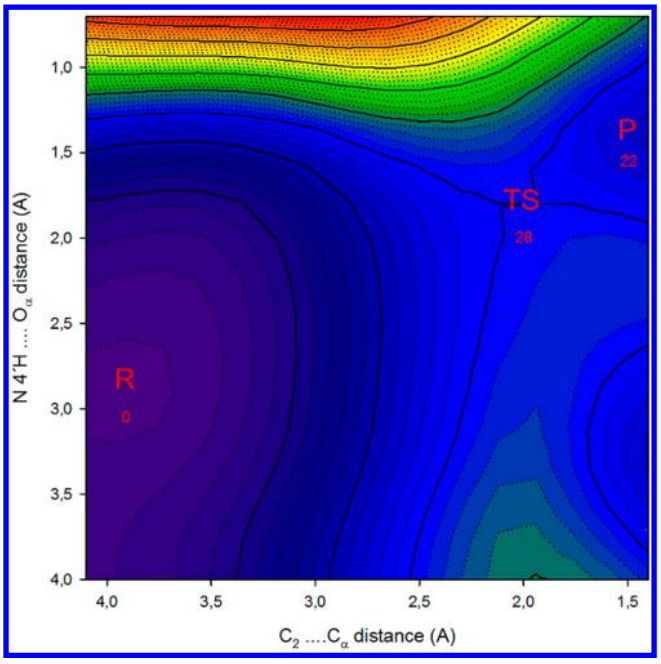

Figure 4. Potential energy surface for the ylide in the AP form.

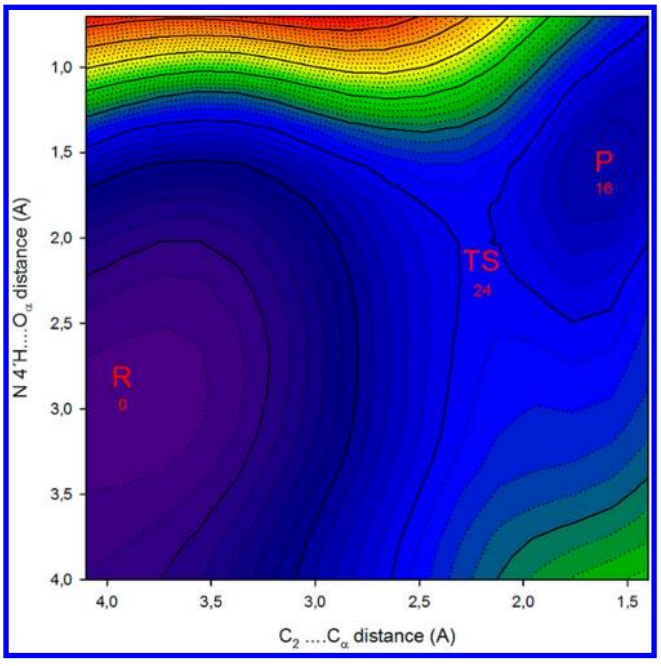

Figure 5. Potential energy surface for the ylide in the APH^+ form.

(R), transition state (TS), and product (P). The reactant state is located at coordinates $R_1 \approx 4.0$ Å and $R_2 \approx 3.0$ Å on the PES. From this point, the PESs show a clear reaction path in which both reaction coordinates vary symmetrically, suggesting a concerted mechanism in which the carboligation and proton transfer occur simultaneously, i.e., while the C_2 atom attacks the carbonyl oxygen of pyruvate, the proton of the N4′ amine group is gradually transferred to the carbonyl oxygen of pyruvate as a consequence of the increasing nucleophilic character on the oxygen atom. The reaction continues in this way until a transition state is reached at coordinates of $R_1 \approx R_2 \approx 2.0$ Å, whose structures are shown in Figures 6 and 7. The important role of the arginine in the stabilization of the transition states by means of the interaction between its

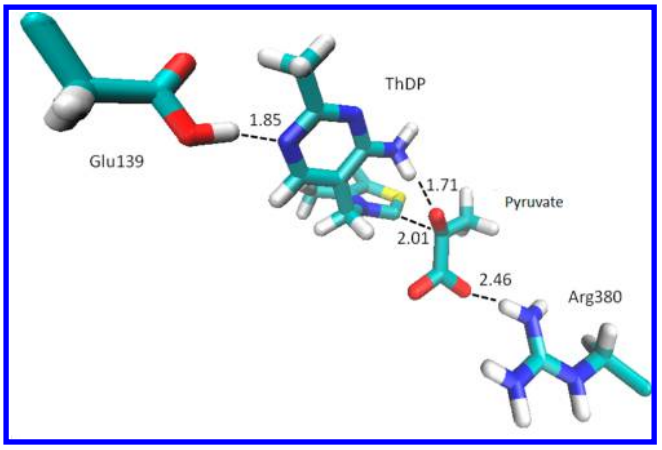

Figure 6. Transition state for the Y_1 form of the ylide. Only the species in the QM region are shown.

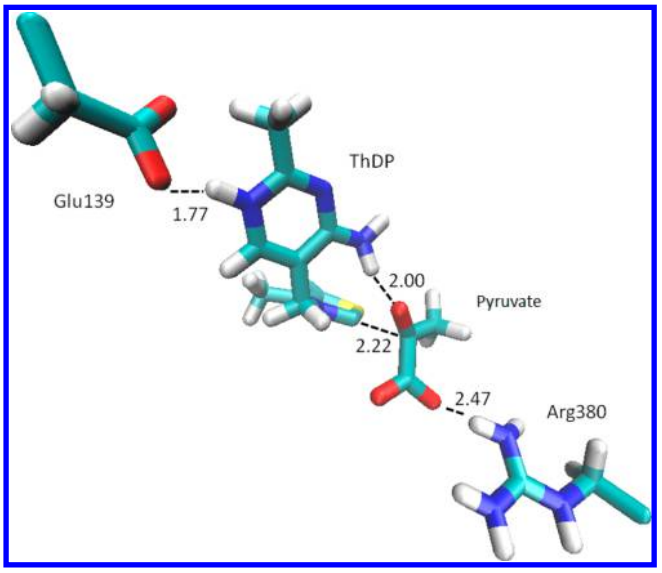

Figure 7. Transition state for the Y_2 form of the ylide. Only the species in the QM region are shown.

guanidium group and the carboxylate group of pyruvate is observed. The associated activation barriers for the two forms of the ylide are 28 and 24 kcal mol^{-1}, respectively. The role of the arginine according to the literature[21] is more relevant in the third step of the catalytic cycle than the first one. This means that the synthesis of L-ThDP is still possible without the presence of this residue, but the observed activation barriers are higher than those observed in the presence of this arginine. In fact, mutation of the arginine is one of the strategies followed for the synthesis of the nonphysiological product R-PAC using AHAS.[21]

Finally, the transition state leads to the product, L-ThDP, located on the PES at coordinates of $R_1 \approx R_2 \approx 1.5$ Å. The product having the N1′ atom protonated is stabilized by 6 kcal mol^{-1} with respect to the other form of the product (N1′ atom deprotonated).

AP−APH^+ Equilibrium. In order to assess the relative stability of the two forms of the ylide, Y_1 and Y_2, we studied the proton transfer from the carboxylic group of the Glu139 residue to the N1′ atom of the 4-aminopyrimidine ring of ThDP. The results show that the Y_2 form (N1′ atom protonated) is stabilized by 4 kcal mol^{-1} with respect to the Y_1 form, and the

DOI: 10.1021/acs.jcim.5b00197
J. Chem. Inf. Model. 2015, 55, 1640−1644

observed activation barrier for this conversion is about 4.5 kcal mol^{-1}.

Energy Diagram. The above results lead to the energy diagram shown in Figure 8, in which the green lines correspond

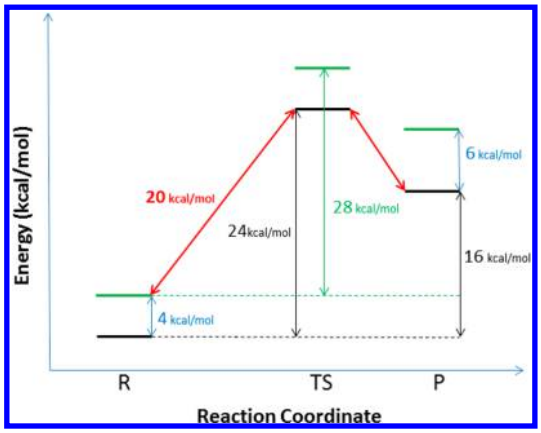

Figure 8. Schematic energy profile for the reaction (red, minimum-energy path; green, Y_1 form of the ylide; black, Y_2 form of the ylide).

to the Y_1 form of the ylide and the black lines correspond to the Y_2 form of the ylide. From this figure it is observed that the activation barriers are 28 and 24 kcal mol^{-1} for the Y_1 and Y_2 forms of the ylide, respectively. Consequently, the reaction to form L-ThDP should occur with the ylide in the Y_2 form, i.e., the form in which the N1′ atom is protonated. However, the diagram also suggests an alternative reaction path having the lowest activation barrier (red line). This hypothetical reaction path of minimum energy would be that in which the reaction begins with the attack of the ylide in its Y_1 form on the C_α atom of pyruvate and reaches a transition state in which the N1′ atom is protonated. In other words, along this postulated minimum-energy reaction path three events occur in a concerted manner, namely, the carboligation, protonation of the N1′ atom by the carboxylic group of the residue Glu 139, and protonation of the carbonyl oxygen of pyruvate by the 4′-amino group.

The conversion from the Y_1 form to the Y_2 form has been confirmed experimentally in solid-state NMR studies.[11] On the other hand, the protonation of the carbonyl oxygen is possible because of the increasing nucleophilic character of this atom triggered by the nucleophilic attack on the carbonyl carbon. This postulated reaction path allows a reduction of the activation barrier to 20 kcal mol^{-1}, in agreement with the experimental evidence.[14]

Analysis of Reactivity. In order to complement the above energetic results, we analyzed the reactivity on key centers as a function of the reaction extent as measured by the approaching distance between pyruvate and the ylide. This was performed by calculating the condensed-to-atom Fukui indices in the gas phase of the species included in the QM region, i.e., pyruvate, the ylide, and the Glu139 and Arg380 residues (Table 1). The results show that the reactivity on the selected atoms depends strongly on the distance between pyruvate and the ylide. At the beginning of the reaction (long C_2-C_α distances), one can observe an important nucleophilic character of the carboxylic oxygens of the Glu139 residue, strong enough to detach the proton from the N1′ atom considering the proximity to the N1′ atom (about 1.8 Å). This fact suggests that in the reactant state the ylide should be in the Y_1 form (N1′ atom deprotonated).

Table 1. Nucleophilic Character on Selected Atoms As Expressed by the f^- Fukui Index

	Y_1		Y_2		
C_2-C_α distance (Å)	C_2	O_α	$GluCOO^-$	C_2	O_α
4.0	0.02	0.00	0.50	0.00	0.00
3.5	0.29	0.02	0.50	0.00	0.00
3.0	0.57	0.04	0.00	0.51	0.07
2.5	0.49	0.11	0.00	0.50	0.12

On the other hand, the f^- Fukui index on the C_2 atom at these early stages of the reaction is null for the Y_2 form of the ylide, conversely to that observed for the Y_1 form. These findings suggest that the reaction is initiated by the ylide in the Y_1 form.

As the reaction progresses and the distance between pyruvate and the ylide becomes shorter, important changes in the Fukui indices are observed. Thus, at approaching distances less than or equal to 3 Å, the nucleophilic character of the carboxylic oxygen becomes null, assuring the sustainability of the ylide in its Y_2 form. On the other hand, the nucleophilicity of the C_2 atom reaches its maximum value, evidencing the nucleophilic attack in progress, which in turn increases the nucleophilic character of the carbonyl oxygen of pyruvate (O_α), in this way allowing the proton abstraction from the amine N4′ atom to form finally the L-ThDP intermediate.

CONCLUSIONS

The results of this study provide a detailed description of the mechanism at different stages of the reaction. The main conclusions can be summarized as follows: (1) The reaction to form L-ThDP occurs via a concerted mechanism in which the carboligation and the proton transfers occur synchronously. (2) The reaction does not occur with only one form of the ylide, Y_1 or Y_2. Instead, both forms participate by means of the conversion of one form (Y_1) to the other form (Y_2) in the course of the reaction. This conversion results in the reaction path of minimum energy, with an activation energy of about 20 kcal mol^{-1}. (3) The approaching distance between pyruvate and the ylide plays a fundamental role in the reaction mechanism since it determines the values of the Fukui reactivity indices on key atoms, which in turn trigger the elemental reactions of the mechanism, namely, carboligation and proton transfers. (4) This interpretation of the reaction mechanism has not been reported earlier in the literature and therefore represents a new approach for the reaction pathway. (5) The results of this study should be valuable for the development of novel herbicides or important pharmaceutical precursors.

AUTHOR INFORMATION

Corresponding Author

*E-mail: edelgado@udec.cl.

Notes

The authors declare no competing financial interest.

ACKNOWLEDGMENTS

Financial support from Grant Fondecyt 1130082 and Doctoral Network UCO 1202 are gratefully acknowledged.

REFERENCES

(1) Zhang, S.; Liu, M.; Yan, Y.; Zhang, Z.; Jordan, J. C2-α-Lactylthiamin Diphosphate is an Intermediate on the Pathway of

DOI: 10.1021/acs.jcim.5b00197
J. Chem. Inf. Model. 2015, 55, 1640−1644

Thiamin Diphosphate-Dependent Pyruvate Decarboxylation. *J. Biol. Chem.* **2004**, *279*, 54312−54318.
(2) Nemeria, N.; Chakraborty, S.; Baykal, A.; Korotchkina, L. G.; Patel, M. S.; Jordan, F. The 1′,4′-Iminopyrimidine Tautomer of Thiamin Diphosphate is Poised for Catalysis in Asymmetric Active Center on Enzymes. *Proc. Natl. Acad. Sci. U. S. A.* **2007**, *104*, 78−82.
(3) Balakrishnan, A.; Gao, Y.; Moorjani, P.; Nemeria, N. S.; Tittmann, K.; Jordan, F. Bifunctionality of the Thiamin Diphosphate Cofactor: Assignment of Tautomeric/Ionization States of the 4′-Aminopyrimidine Ring when Various Intermediates Occupy the Active Sites During Catalysis of Yeast Pyruvate Decarboxylase. *J. Am. Chem. Soc.* **2012**, *134*, 3873−3885.
(4) Agyei-Owusu, K.; Leeper, F. J. Thiamin Diphosphate in Biological Chemistry: Analogues of Thiamin Diphosphate in Studies of Enzymes and Riboswitches. *FEBS J.* **2009**, *276*, 2905−2916.
(5) Kluger, R.; Tittmann, K. Thiamin Diphosphate Catalysis: Enzymic and Nonenzymic Covalent Intermediates. *Chem. Rev.* **2008**, *108*, 1797−1833.
(6) Nemeria, N. S.; Chakraborty, S.; Balakrishnan, A.; Jordan, F. Reaction Mechanisms of Thiamin Diphosphate Enzymes: Defining States of Ionization and Tautomerization of the Cofactor at Individual Steps. *FEBS J.* **2009**, *276*, 2432−2446.
(7) Jordan, F.; Nemeria, N. S. Experimental Observation of Thiamin Diphosphate-Bound Intermediates on Enzymes and Mechanistic Information Derived from These Observations. *Bioorg. Chem.* **2005**, *33*, 190−215.
(8) Widmann, M.; Radloff, R.; Pleiss, J. The Thiamine Diphosphate Dependent Enzyme Engineering Database: a Tool for the Systematic Analysis of Sequence and Structure Relations. *BMC Biochem.* **2010**, *11*, No. 9.
(9) Gocke, D.; Walter, L.; Gauchenova, E.; Kolter, G.; Knoll, M.; Berthold, C. L.; Schneider, G.; Pleiss, J.; Müller, M.; Pohl, M. Rational Protein Design of ThDP-Dependent Enzymes-Engineering Stereoselctivity. *ChemBioChem* **2008**, *9*, 406−412.
(10) Knoll, M.; Müller, M.; Pleiss, J.; Pohl, M. Factors Mediating Activity, Selectivity, and Substrate Specifity for the Thiamin Diphosphate-Dependent Enzymes Benzaldehyde Lyase and Benzoylformate Decarboxylase. *ChemBioChem* **2006**, *7*, 1928−1934.
(11) Balakrishnan, A.; Paramasivam, S.; Chakraborty, S.; Polenova, T.; Jordan, F. Solid-State Nuclear Magnetic Resonance Studies Delineate the Role of the Protein in Activation of Both Aromatic Rings of Thiamin. *J. Am. Chem. Soc.* **2012**, *134*, 665−672.
(12) Paramasivam, S.; Balakrishnan, A.; Dmitrenko, O.; Godert, A.; Begley, T. P.; Jordan, F.; Polenova, T. Solid State NMR and Density Functional Theory Studies on Ionization States of Thiamin. *J. Phys. Chem. B* **2011**, *115*, 730−736.
(13) Jaña, G. A.; Delgado, E. J. Electron Density Reactivity Indexes of the Tautomeric/Ionization Forms of Thiamin Diphosphate. *J. Mol. Model.* **2013**, *19*, 3799−3803.
(14) Alvarado, O.; Jaña, G.; Delgado, E. J. Computer-Assisted Study on the Reaction Between Pyruvate and Ylide in the Pathway Leading to Lactyl-ThDP. *J. Comput.-Aided Mol. Des.* **2012**, *26*, 977−982.
(15) Sanchéz, L.; Jaña, G. A.; Delgado, E. J. A QM/MM Study on the Reaction Pathway Leading to 2-Aceto-2-Hydroxybutyrate in the Catalytic Cycle of AHAS. *J. Comput. Chem.* **2014**, *35*, 488−494.
(16) Jaña, G.; Jimenez, V.; Villa-Freixa, J.; Prat-Resina, X.; Delgado, E.; Alderete, J. B. A QM/MM Study on the Last Two Steps of the Catalytic Cycle of Acetohydroxyacid Synthase. *Comput. Theor. Chem.* **2011**, *966*, 159−166.
(17) Hermann, J. C.; Hensen, C.; Ridder, L.; Mulholland, A. J.; Höltje, H.-D. Mechanisms of Antibiotic Resistance: QM/MM Modeling of the Acylation Reaction of a Class A β-Lactamase with Benzylpenicillin. *J. Am. Chem. Soc.* **2005**, *127*, 4454−4465.
(18) Brooks, B. R.; Brooks, C. L., III; Mackerell, A. D., Jr.; Nilsson, L.; Petrella, R. J.; Roux, B.; Won, Y.; Archontis, G.; Bartels, C.; Boresch, S.; Caflisch, A.; Caves, L.; Cui, Q.; Dinner, A. R.; Feig, M.; Fischer, S.; Gao, J.; Hodoscek, M.; Im, W.; Kuczera, K.; Lazaridis, T.; Ma, J.; Ovchinnikov, V.; Paci, E.; Pastor, R. W.; Post, C. B.; Pu, J. Z.; Schaefer, M.; Tidor, B.; Venable, R. M.; Woodcock, H. L.; Wu, X.; Yang, W.; York, D. M.; Karplus, M. CHARMM: The Biomolecular Simulation Program. *J. Comput. Chem.* **2009**, *30*, 1545−1614.
(19) Shao, Y.; Molnar, L. F.; Jung, Y.; Kussmann, J.; Ochsenfeld, C.; Brown, S. T.; Gilbert, A. T. B.; Slipchenko, L. V.; Levchenko, S. V.; O'Neill, D. P.; DiStasio, D. A., Jr.; Lochan, R. C.; Wang, T.; Beran, G. J. O.; Besley, N. A.; Herbert, J. M.; Lin, C. Y.; Van Voorhis, T.; Hung Chien, S.; Sodt, A.; Steele, R. P.; Rassolov, V. A.; Maslen, P. E.; Korambath, P. P.; Adamson, R. D.; Austin, B.; Baker, J.; Byrd, E. F. C.; Dachsel, H.; Doerksen, R. J.; Dreuw, A.; Dunietz, B. D.; Dutoi, A. D.; Furlani, T. R.; Gwaltney, S. R.; Heyden, A.; Hirata, S.; Hsu, C. P.; Kedziora, G.; Khalliulin, R. Z.; Klunzinger, P.; Lee, A. M.; Lee, M. S.; Liang, W. Z.; Lotan, I.; Nair, N.; Peters, B.; Proynov, E. I.; Pieniazek, P. A.; Rhee, Y. M.; Ritchie, J.; Rosta, E.; Sherrill, C. D.; Simmonett, A. C.; Subotnik, J. E.; Woodcock, H. L., III; Zhang, W.; Bell, A. T.; Chakraborty, A. K.; Chipman, D. M.; Keil, F. J.; Warshel, A.; Hehre, W. J.; Schaefer, H. F., III; Kong, J.; Krylov, A. I.; Gill, P. M. W.; Head-Gordon, M. Advances in Methods and Algorithms in a Modern Quantum Chemistry Program Package. *Phys. Chem. Chem. Phys.* **2006**, *8*, 3172−3191.
(20) *Jaguar*, version 7.7; Schrödinger, LLC: New York, 2010.
(21) Engel, S.; Vyazmensky, M.; Vinogradov, M.; Berkovich, D.; Bar-Ilan, A.; Qimron, U.; Rosiansky, Y.; Barak, Z.; Chipman, D. M. Role of a Conserved Arginine in the Mechanism of Acetohydroxy Synthase. *J. Biol. Chem.* **2004**, *279*, 24803−24812.

DOI: 10.1021/acs.jcim.5b00197
J. Chem. Inf. Model. 2015, 55, 1640−1644